

THE SOLAR RADIO CORONA: MANIFESTATIONS OF ENERGETIC ELECTRONS

(Invited)

Monique Pick

Observatoire de Paris-Meudon, DASOP, UA 324

I. INTRODUCTION

Most of the topics I am going to discuss in this talk concern the acceleration of particles during solar flares. The energy transferred to particles is in fact a great fraction of the energy released during a flare; hence, the problems related to the acceleration/injection process are of crucial importance for build-up and evolution of the flare.

The accelerated particles produce a wide variety of electromagnetic radiation including hard X-ray and radio bursts. The various kinds of emissions are generated in the corona through different mechanisms in sources with different physical parameters. Hence, any common feature in the temporal evolution of the fluxes can be attributed to the energetic particles. Furthermore, the different heights of emission enable us to deduce information on the three-dimensional structure of the source region from imaging observations in hard X rays, microwaves, and meter waves. One of the best prospects for understanding the electron acceleration has recently emerged from observations of X-ray and radio emission with a time resolution of ≤ 1 s. A detailed comparison of source locations and temporal evolution at different wavelengths is an important means to investigate crucial problems of the flare development such as:

- The temporal evolution of the electron population in the sources under the influence of acceleration/injection and interaction with the ambient medium.
- The magnetic structure involved in the acceleration/injection site.
- The alternative between long-term particle storage in the corona and continuous or repetitive injection.

My talk will be divided into two chapters: The first one deals with the solar flare development: pre-impulsive and impulsive phases, gradual and post gradual phases. A few points related to electron acceleration outside of flares will be also briefly discussed. The second chapter concerns a few problems related to the radio emission processes.

II. THE SOLAR FLARE DEVELOPMENT: PARTICLE ACCELERATION DURING AND OUTSIDE OF FLARES

(a) Impulsive phase

It is well accepted that electrons responsible for type III bursts and hard X-ray emission have a common origin. This idea is based on the temporal association between these emissions, when they are both produced. In fact, Raoult et al. (1985) have shown that the hard X-ray bursts associated with metric type III (or U) groups are of moderately small importance. They have a peak flux $\leq 1 \text{ ph cm}^{-2} \text{ s}^{-1} \text{ keV}^{-1}$ at about 30 keV. On the opposite, X-ray bursts associated with type III/V emission lasting more than 30 s are considerably more intense with peak

fluxes around 30 keV exceeding $1 \text{ ph cm}^{-2} \text{ s}^{-1} \text{ keV}^{-1}$ and spectra extending to $\geq 100 \text{ keV}$. The study of the spatial and temporal characteristics of type III/V events as well as their temporal association with X-ray emission came out with new information on the development of the impulsive phase. The observations (see Figures 1a and 1b) can be summarized as follows:

— There is an overall temporal correlation between X-ray and radio emissions. As X rays are produced in dense regions, this correlation implies a quasi-continuous input of accelerated electrons in the corona.

— In the early stage of the event, during the pre-impulsive phase which is shorter than 1 min, radio emission is primarily type III or U bursts, the type III bursts arising from several locations. The X-ray flux ($\leq 1 \text{ ph cm}^{-2} \text{ s}^{-1} \text{ keV}^{-1}$ at 30 keV, similar to pure type III flare events) grows as the type III frequency increases. This effect is frequently observed. As the radiation of the type III bursts is emitted at the local plasma frequency or its harmonic, the starting frequency corresponds to the density at the point where the electron beams become unstable. Thus, the fast variation of the starting frequency may be explained by a real variation of the electronic density in the source (downward shift or compression of the injection/acceleration site) (Kane and Raoult, 1981). Alternatively, this effect may be linked to a variation in the distance traveled by the electron beam from the acceleration site before it becomes unstable to plasma waves (Kane et al. 1982).

— During the fast increase of the X-ray flux, one of the type III sources labeled A' in Figure 1 becomes predominant and a new different source B appears. These two sources fluctuate together with short time delays of often less than 1 s. Both sources contribute together to the spiky (burst) and smooth continuum part of the radio emission. The simplest interpretation of the behavior of these two sources is that fast electrons are injected simultaneously into two magnetic structures as illustrated in Figure 2. This can happen if two magnetic structures suddenly interact at the acceleration/injection site. Several other observations give complementary information.

Microwave observations show effectively the electron propagation inside an arch. Indeed, they have revealed the existence of secondary bursts occurring at distances of 10^5 to 10^6 km from the primary site (Nakajima et al., 1985). The secondary burst has a time profile similar to the primary burst with a delay of 2 to 25 s. Some of these events occur simultaneously with meter-wave type III/V bursts. These observations strongly suggest that the distant microwave burst is produced by 10 to 100 keV electrons channeled along a coronal loop from the flare site to the distant footpoint of the loop.

Analysis of soft and hard X-ray imaging observations obtained with HXIS aboard SMM or with Hinotori also support the evidence of two systems of loops interacting. As an example, for one event, on 29 June 1980 associated with type III/V emission, different components of the X-ray source have been resolved. These features are labeled A, B, C, and D in Figure 2d (Hernandez et al., 1985). Feature A is a small loop (length $< 20\,000$ km). Features B and C are located in a large loop system, C corresponding to the footpoint, and B to a coronal source. The spatial configuration strongly suggests that the radio source B is the counterpart of the coronal X-ray source B. Furthermore, feature D which looks like a surge-like structure is located in the interaction volume of the 2 loops and its temporal behavior (Figure 3) reveals that the maximum of *thermal* energy release occurs in this region. Similar surges have been observed in H α , and a systematic study has proved the close association between the appearance of these surges and type III burst occurrence (Mein and Avignon, 1985; Chiuderi-Drago et al., 1985):

there is a relationship between the evolution of the velocities of the H α dark material and the occurrence of the type III bursts; the radio emission occurs in coincidence, within 1 min, with the blueshift maxima. The production of these surges may be due to the interaction volume which induces compression and thermal instability (Poland et al., 1982).

In conclusion, major progress has been achieved in the understanding of the impulsive development. Nevertheless, with the instruments presently available, it is difficult to achieve properly a quantitative interpretation. X-ray instruments with improved sensitivity and spatial resolution are necessary. Indeed, during the pre-impulsive phase, the comparative study between the temporal evolution of the X-ray spectrum and the radio emission cannot be carried out presently. Similarly, the time resolution of the X-ray image is too poor to obtain the exact evolution of the different features and their temporal association. In particular, we do not know if the bright points at the foot of the flaring loop appear simultaneously. Finally, the spatial resolution is insufficient to understand the exact topology of the accelerating site, and how, for example, electrons can be injected along several discrete diverging magnetic paths. The mechanism of electron acceleration that takes place is not yet understood. For this purpose, I would like to mention now the potential interest of radio decimeter observations.

Spikes of duration less than 100 ms are frequently observed above the starting frequency of type III bursts. An example is shown in Figure 4 together with a hard X-ray time profile for comparison (Benz, 1985). The spikes tend to occur in the early phase of the type III groups and predominantly in the rising phase of hard X rays. The most plausible interpretation is emission at the electron cyclotron frequency or harmonic (upper hybrid wave emission or cyclotron maser) (Benz, 1985). Figure 5 displays the temporal evolutions of average spike flux, metric type III flux, and hard X-ray counting rate. The observed correlation clearly demonstrates the close connection between spikes and the injection of energetic electrons. Following Benz, the spikes originate close to, or in the energy release region. "The observed fragmentation of the decimetric radiation into spikes might be a secondary effect of one global energy release or it could reflect that the energy of flares is released in thousands of 'microflares' (typical energy $\cong 10^{26}$ ergs)." The latter interpretation suggests that type III bursts may be related to integrated effects of elementary acceleration events during the solar flares (Benz, 1985).

All the observations shown here have pointed out the quasi-continuous and nearly simultaneous injection of electrons into distinct magnetic structures (type III/V emission) and precipitating, at least partially, electrons associated with hard X-rays bursts. The accelerating region must share different diverging field lines (Kane et al., 1980). Another possibility, proposed by Sprangle and Vlahos (1983), is the acceleration of secondary electrons generating type III bursts by intense radio waves. The signature of these radio waves is given by the presence of decimetric bursts. In this model, the "flaring loop model," the primary accelerated electrons are produced in the flaring loop, and excite the e.m. radio waves which can easily escape from the flaring region.

It must be indicated that joint observations obtained with a multifrequency radiohelio-graph and the hard X-ray imaging instrument of the Pinhole/Occulter Facility will provide in principle an answer to this problem. Indeed, the respective location of the spike and type III bursts will be obtained as well as the hard X-ray source structure.

(b) Gradual and late phases of large solar flares

It is now widely accepted that during the gradual phases of large solar flares, the electrons are continuously or repetitively injected into different coronal structures where they emit hard X rays and broadband continua from centimeter to meter radio waves (Kai et al., 1983; Hudson et al., 1982; Klein et al., 1983). The strongest argument supporting this conclusion is the similarity of time profiles between hard X rays, microwaves, and meter emissions.

Despite this general agreement several problems still remain confused. First of all, it seems to me that a great deal of ambiguity arises from the inhomogeneous terminology adopted by different authors to describe the successive stages of type IV events. This led some authors to suggest an association between hard X-ray emission and, indifferently, "flare continuum" or late "stationary type IV burst" without any clear distinction between these two components. The consequence has been a confusion in the electron energy responsible for the different components of a type IV burst. Secondly, type II bursts which are produced by shock waves are often observed at the onset of type IV bursts. The exact role of shocks in the acceleration of electrons responsible for type IV emission is not yet understood.

A typical radio observation of a big solar flare is shown in Figure 6. Let me recall that:

(1) The gradual phase comprises a broadband emission from centimeter to meter waves that often starts during the impulsive phase. This part, very well-observed at single frequencies called "flare continuum" (Wild, 1970), has in general a duration of a few tens of minutes, exceeding sometimes one hour for large events (Pick, 1961; the "phase A" in this paper is identical to the term "flare continuum"). Sometimes this emission is accompanied by a "moving type IV burst" at meter waves. This is in contradiction with what was reported later on by Cliver (1983). This author had in mind that the flare continua are of short duration, and he designated as stationary type IV burst events that were in fact typical flare continua extending to microwave frequencies.

(2) The post gradual phase, "stationary type IV burst," corresponds to a long lasting emission up to many hours at meter decameter wavelengths and occurs in some flares during the fading of the flare continuum or sometimes without any proceeding impulsive or gradual phase.

Figures 7 and 8 compare the temporal evolution of hard X-ray and radio emissions between two flares containing a flare continuum which starts at the time of the impulsive phase emission. Flare continuum and hard X-ray emissions start and finish together, presenting an overall similar temporal behavior. The observed nearly simultaneous end of the burst and of some of its fine structure features, in both spectral ranges, indicates that the electrons are not efficiently trapped. The electrons must be quasi-continuously injected.

Furthermore, one can notice that for the 13 August 1980 event (Figure 8), the onset of the flare continuum at meter wavelengths clearly occurs during the flash phase, *before* the type II burst occurrence. Thus, it is not classified as FCII continua which are initiated by the passage of the shock wave accelerating *locally* the electrons (Robinson and Smerd, 1975) (see also Figure 9). On the other hand, Hudson et al. (1982) associated a hard X-ray event with an FCII flare continuum. They suggested that the timings of the FCII, the X-ray, and microwave emissions were all consistent with the shock wave as the accelerating agent. Then, it is not understandable that the onset of the hard X-ray event lagged significantly behind the appearance of the type II burst and the 80 MHz continuum (Figure 10). Hudson et al. (1982) suggested that the particle acceleration site is largely remote from the impulsive first-stage energy release, contrary to other major flares. As the corresponding flare occurs behind the limb, I suggest that a large part of the gradual X-ray event may be occulted as well as the impulsive phase. Indeed, Kane (1983) has shown that, for impulsive and gradual bursts, the bulk of hard X rays is below 3000 km.

Occasionally, for disk events a delay between X-ray and radio emissions has been observed. The onset of X-ray bursts precedes the onset of the meter radio emission.

In conclusion and for discussion:

- (a) Flare continua are produced by energetic electrons.
- (b) The temporal relationship between X-ray emission and flare continuum has still to be clarified. It is indeed not clear enough whether two physically distinct accelerating mechanisms exist; one corresponding to an injection/accelerating site located relatively low in the corona and producing electrons continuously or repetitively during the whole development of the event; another one corresponding to an *in situ* accelerating process linked for a given altitude to the passage of the shock wave. Robinson himself, who introduced the distinction between FCM and FCII flare continua, notices that “the type FCII activity is accompanied by an unclassified continuum burst sometimes having the properties of the type III/V” (Figure 11) (Robinson, 1977). I suggest that the energetic electrons responsible for FCII events may be also produced in the lower levels of the solar atmosphere, close to the site of flare energy release. Kundu and Stone concluded similarly for the kilometric solar radio bursts detected by Cane et al. (1981) and referred to them as shock-accelerated (SA) events (Kundu and Stone, 1984).
- (c) The source topology during both impulsive and gradual phases looks roughly similar. Both phases require a quasi-continuous acceleration mechanism. Despite this analogy, we do not yet understand why some large flares are only associated with relatively short type III/V events (plausibly “flare of class B” in the Hinotori classification) and others with “flare continua” of longer duration (plausibly “flares of class C” in the Hinotori classification). The mechanism maintaining a continuous input of energy from the interaction region is still unknown.
- (d) One of the important results coming out from the SMM mission is that protons and heavy ions are rapidly accelerated during the impulsive phase (Forrest et al., 1981; Chupp, 1982). It was suggested that all flares might produce γ -ray lines and that only the threshold sensitivity distinguishes the gamma-ray line flares from the others. On the opposite, Bai and Dennis argued that γ -ray line events exhibit distinct characteristics from other flares. They concluded that these events belong to a distinct class of flares (Bai and Dennis, 1985). One of the characteristics is the close association between type II/IV bursts and γ -ray line events. Let me emphasize the fact that an *association* between two features has not the same meaning as a “temporal correlation.” In that way, it must be noticed that the 3 June 1982 flare, one of the most important γ -ray line events observed by SMM, showed 3 successive blobs of activity, comparable to 3 type V events (Figure 12) followed by a type IV event. The onset and the development of the γ -ray emission occurs during the first type V burst. On the other hand, Raoult et al. (1985) notice that γ -ray events may occur in association with type III/V events and in the absence of any type IV burst.

The Post Gradual Phase

When the gradual meter emission is followed by a storm continuum (stationary type IV burst), the latter is not associated with detectable hard X rays, but only with soft ones (Stewart, Wolfson, and Lemen, 1979; Svestka et al., 1982; Klein et al., 1983). An isolated storm continuum has been observed by Lantos et al. (1981), with spatial resolution in the meter and soft X-ray range. Although the sources are widely separated, their fluxes evolve in the same manner. Lantos et al. proposed that electrons of about 10 keV in the tail of the thermal distribution emitting soft X rays escape from the X-ray source and generate the radio emission inside a large expanding loop transient.

(c) *Electron acceleration outside of flares*

(1) Micro-activity at meter decameter wavelengths

Using a balloon-borne instrumentation of very high sensitivity, Lin et al. (1984) have detected many hard X-ray microbursts, 25 in 141 min, with peak fluxes exceeding 7×10^{-3} ph cm $^{-2}$ s $^{-1}$ keV $^{-1}$ at 20 keV and with a power-law energy spectrum. H α flares were only reported for a few of the strongest bursts. The integral number of events varies approximately as the inverse of the peak flux (Figure 13). Lin et al. concluded that the energy contained in accelerated electrons might contribute significantly to the heating of the active corona. Kundu and Stone (1984) proposed that these microbursts could be of the same nonthermal nature as the frequent microbursts observed at meter and decameter wavelengths. The CLRO radioheliograph recorded many micro-type-III-like bursts lasting from a few seconds to several tens of seconds with flux densities ranging from a few tens to hundreds of milli sfu. As shown by Kundu and Stone, the integral number of events also varies inversely to the peak flux (Figure 13). The Clark Lake Radioheliograph images show that the radio source persists for many hours. These type-III-like burst storms are also frequently observed at higher frequencies as weak meter type I noise storms. The exact origin of the electrons responsible for these emissions is not yet understood.

(2) Noise storm onsets or enhancements related to transient coronal modifications

The most rapid variations of the K corona, coronal transients, have been extensively studied, and some of them are known to be associated with type II-IV bursts (for a review, see the chapter on "coronal mass ejections and coronal structures" by Hildner et al. in the SMM workshop proceedings, 1985). I am not going to discuss these large events here.

Combining SMM - C/P observations and Nançay Radioheliograph measurements, Kerdraon et al. (1983) found that noise storm onsets or enhancements are systematically associated with the appearance of additional material in the corona. These coronal brightenings are not necessarily transient mass ejections. Most often, they appear as a stepwise increase on a timescale of one hour and remain stable for several hours. In all cases, the radio source is cospatial with the region of increased white light brightness. Whatever may be the process causing the mass increase, it is a necessary condition for the noise storm emission to change intensity or to appear. This result represents the first systematic association between visible features and noise storm production. Indeed, attempts to associate this activity with chromospheric flares (Elgaroy, 1977) or with surges (Garczynska et al., 1982) did not reveal any systematic relationship.

In conclusion, electrons can be accelerated quasi-continuously in the absence of any detectable chromospheric activity. The observations summarized in this section may suggest that these electrons may have a purely coronal origin. In order to progress, joint observations between radioheliographs, white-light and UV coronographs, especially observing below 1.5 solar radii from disk center, are necessary to establish more clearly this coronal origin.

III. RADIO EMISSION PROCESSES AND ELECTRON BEAM OBSERVATION

(a) *Type III radio bursts*

In the last years, both theory and observational techniques of solar type III bursts have been developed up to a level where it became possible to investigate the fine structure of type III radio emission and to use it as a test of the theory. At kilometric wavelengths, pioneering work in this direction has been done by Lin et al. (1973), Gurnett and Anderson (1976), and

Fitzenreiter et al. (1976) from an observational point of view, and by Goldstein et al. (1979) from a theoretical point of view. For example, it was possible to confirm that the radio emission is produced by streaming electrons. In the higher frequency band, *in situ* verification of the theory is not possible. Indirect investigation by means of the radio emission has been the appropriate way to get information about the early development of the electron beams. The conclusions diverge significantly. On the other hand, many authors have invoked propagation effects of electromagnetic waves, such as coronal scattering or wave ducting to explain observed size, position, directivity, and characteristics of fundamental-harmonic pairs (F-H) (Steinberg et al., 1971; Stewart, 1976; Duncan, 1980; Dulk and Suzuki, 1980). On the other hand, other authors have noted that type III bursts may be resolved into elementary sources which can be explained by the discrete diverging structures in the corona (Axisa et al., 1972; Mercier, 1975; Raoult and Pick, 1980). This was recently confirmed by direct combined white-light and radio observations obtained with the SMM coronograph/polarimeter and the Nançay Radioheliograph. It was shown that type III sources are located in the vicinity of thin ray-like structures which are over-dense, short-lived (1 day or less), and sometimes diverging (Trottet et al., 1982). More generally, the type III source structure tends to follow that of the corona. Even if propagation effects are not excluded, they must be estimated in the context of a corona composed of small discrete structures. This has direct implication on the type III burst modeling. For example, type III pairs are often observed; most of the observed type III pairs have been widely interpreted as fundamental and harmonic emission (F-H). However, this interpretation may sometimes encounter serious difficulties as the observations fit occasionally better with the assumption of 2 electron beams propagating along different diverging magnetic paths (Benz et al., 1982).

In *situ* measurements of electron beams in connection with coronal observations will yield powerful diagnostics of the radio emitting mechanisms. Indeed, electron beam propagation characteristics will be clearly identifiable and distinguishable from propagation effects of electromagnetic waves. Finally, it must be emphasized that results which have been obtained from *in situ* measurements at low frequencies in the interplanetary medium cannot be automatically extrapolated to higher radio frequencies emitted at coronal levels.

(b) Pulsating structure

Flux variations with quasi-periods of the order of 1 s are frequently observed in type IV continua (McLean et al., 1971). They are referred to as "pulsating structure." Theories involving incoherent or coherent gyrosynchrotron radiation from energetic electrons trapped in a magnetic arch and periodic oscillations of this arch have been often invoked for the interpretation of pulsating structure (Rosenberg, 1970).

Combined imaging and spectral observations have made a detailed study possible of both the spatial structure of the source and its emission spectrum. This led to the discovery of new properties of these modulations as high temperatures $\sim 10^{11}$ K, limited frequency spectrum, spatial and spectral drift of the peak frequency within one pulse (Trottet et al., 1981). It has been shown that these characteristics exclude gyrosynchrotron radiation as the emission mechanism. As an alternative, processes where the plasma emission of trapped particles is inhibited by perturbations of the loss cone distribution have been proposed. These perturbations can correspond to repetitive injections of fast electrons as suggested by Benz and Kuijpers(1976) for the interpretation of "sudden reductions" in continua. As mentioned by Trottet et al., "simultaneous X-ray and radio observations of similar pulsating structure events will furnish clues concerning the changes in distribution function and the correctness of the model."

IV. CONCLUSIONS

Radio observations are powerful tools which are complementary to the space missions devoted to the physics of the flares, of the corona, or of the interplanetary medium. I would like to take this opportunity to stress the fact that two multifrequency radioheliographs presently exist: the Nançay instrument (the multifrequency facility will be in operation by the end of 1985) observes the middle corona at decimeter-meter wavelengths, and the Clark Lake radioheliograph, operating at decameter wavelengths, is the only one in the world to have the ability of observing the outer corona above the disk.

Acknowledgments. I acknowledge L. Klein, A. Raoult, G. Trottet, and N. Vilmer for helpful discussions and criticisms on the manuscript.

REFERENCES

- Axisa, F., Martres, M. J., Pick, M., and Soru-Escaut, I., 1972, Goddard, NASA Symposium.
- Bai, T. and Dennis, B. R., 1985, *Astrophys. J.*, in press.
- Benz, A., 1985, *Solar Phys.*, **96**, 357.
- Benz, A. O. and Kuijpers, J., 1976, *Solar Phys.*, **46**, 275.
- Benz, A. O. Treumann, R., Vilmer, N., Mangeney, A., Pick, M., and Raoult, A., 1982, *Astron. Astrophys.*, **108**, 161.
- Cane, H. V., Stone, R. G., Fainberg, J., Stewart, R. T., Steinberg, J. L., and Hoang, S., 1981, *Geophys. Res. Lett.*, **8**, 1285.
- Chiuderi-Drago, F., Mein, N., et al., 1985, in preparation.
- Chupp, E. L., 1982, in *Gamma Ray Transients and Related Astrophysical Phenomena*, ed., R. A. Lingenfelter, New York, p. 409.
- Cliver, E. W., 1983, *Solar Phys.*, **84**, 347.
- Datlowe, D. W., Elcan, M. J., and Hudson, H. S., 1974, *Solar Phys.*, **39**, 155.
- Dulk, G. A. and Suzuki, S., 1980, *Astron. Astrophys.*, **80**, 203.
- Duncan, R. A., 1980, *Solar Phys.*, **63**, 389.
- Elgaroy, O., 1977, *Solar Noise Storms*, ed., D. Ter Haar, New York, Pergamon Press.
- Fitzenreiter, R. J., Evans, L. G., and Lin, R. P., 1976, *Solar Phys.*, **46**, 437.
- Forrest, D. J., et al., 1981, in *Proc. 17th Intl. Cosmic Ray Conf. (Paris)*, **10**, 5.
- Garczynska, I., Rompolt, B., Benz, A., Slottje, C., Tlamicha, A., and Zanelli, C., 1982, *Solar Phys.*, **77**, 277.
- Goldstein, M. L., Smith, R. A., and Papadopoulos, K., 1979, *Astrophys. J.*, **234**, 683.
- Gurnett, O. A. and Anderson, R. R., 1976, *Science*, **194**, 1159.
- Hernandez, A. M., Machado, M. E., Sneibrun, C. V., Trottet, G., and Vilmer, N., 1985, to be submitted.
- Hildner, E., et al., 1985, in Proceedings of the SMM Workshop.
- Hudson, H. S., Lin, R. P., and Stewart, R. T., 1982, *Solar Phys.*, **75**, 245.
- Kai, K., Nakajima, H., Kosugi, T., and Kane, S. R., 1983, *Solar Phys.*, **86**, 231.
- Kane, S. R., 1983, *Solar Phys.*, **86**, 355.
- Kane, S. R., Pick, M., and Raoult, A., 1980, *Astrophys. J. (Letters)*, **241**, L113.
- Kane S. R. and Raoult, A., 1981, *Astrophys. J. (Letters)*, **248**, L77.
- Kane, S. R., Benz, A. O., and Treumann, R. A., 1982, *Astrophys. J.*, **263**, 423.
- Kerdraon, A., Pick, M., Trottet, G., Sawyer, C., Illing, R., Wagner, W., and House, L., 1983, *Astrophys. J. (Letters)*, **265**, L19.
- Klein, L., Anderson, K., Pick, M., Trottet, G., and Vilmer, N., 1983, *Solar Phys.*, **84**, 295.
- Kundu, M. R. and Stone, R. G., 1984, *Advances in Space Research*, ed., P. A. Simon, **4**, 261.
- Lantos, P., Kerdraon, A., Rapley, C. G., and Bentley, R. D., 1981, *Astron. Astrophys.*, **101**, 33.
- Lin, R. P., Evans, L. G., and Fainberg, J., 1973, *Astrophys. Letters*, **14**, 191.
- Lin, R. P., Schwartz, R. A., Kane, S. R., Pelling, R. M., and Hurley, K. C., 1984, *Astrophys. J.*, **283**, 421.
- McLean, D. J., Sheridan, K. V., Stewart, R. T., and Wild, J. P., 1971, *Nature*, **234**, 140.
- Mein, N. and Avignon, Y., 1985, *Solar Phys.*, **95**, 2, 331.
- Mercier, D., 1975, *Solar Phys.*, **45**, 169.
- Nakajima, H., Dennis, B. R., Hoyng, P., Nelson, G., Kosugi, T., and Kai, K., 1985, *Astrophys. J.*, **288**, 806.
- Newkirk, G., 1961, *Astrophys. J.*, **133**, 983.
- Pick, M., 1961, *Ann. Astrophys.*, **24**, 183.
- Poland, A. I., Machado, M. E., Wolfson, C. J., Frost, K. J., Woodgate, B. E., Shine, R. A., Keny, P. J., Cheng, C. C., Tandberg-Hanssen, E. A., Bruner, E. C., and Henze, W., 1982, *Solar Phys.*, **78**, 201.

- Raoult, A. and Pick, M., 1980, *Astron. Astrophys.*, **87**, 63.
- Raoult, A., Pick, M., Dennis, B. R., and Kane, S. R., 1985, *Astrophys. J.*, submitted.
- Robinson, R. D. and Smerd, S. F., 1975, *Proc. A.S.A.*, **2**, 374.
- Robinson, R. D., 1977, Thesis.
- Rosenberg, H., 1970, *Astron. Astrophys.*, **9**, 159.
- Sprangle, P. and Vlahos, L., 1983, *Astrophys. J. (Letters)*, **273**, L95.
- Steinberg, J. L., Aubier-Giraud, M., Leblanc, Y., and Boischot, A., 1971, *Astron. Astrophys.*, **10**, 362.
- Stewart, R., 1976, *Solar Phys.*, **50**, 437.
- Stewart, R., Wolfson, C. J., and Lemen, J. R., 1979, *NZJS*, **22**, 567.
- Svestka, Z., Dennis, B. R., Pick, M., Raoult, A., Rapley, C. G., Stewart, R. T., and Woodgate, B. E., 1982, *Solar Phys.*, **80**, 143.
- Trottet, G., Kerdraon, A., Benz, A. O., and Treumann, R., 1981, *Astron. Astrophys.*, **93**, 129.
- Trottet, G., Pick, M., House, L., Illing, R., Sawyer, C., and Wagner, W., 1982, *Astron. Astrophys.*, **111**, 306.
- Wild, J. P., 1970, *Proc. A.S.A.*, **1**, 365.

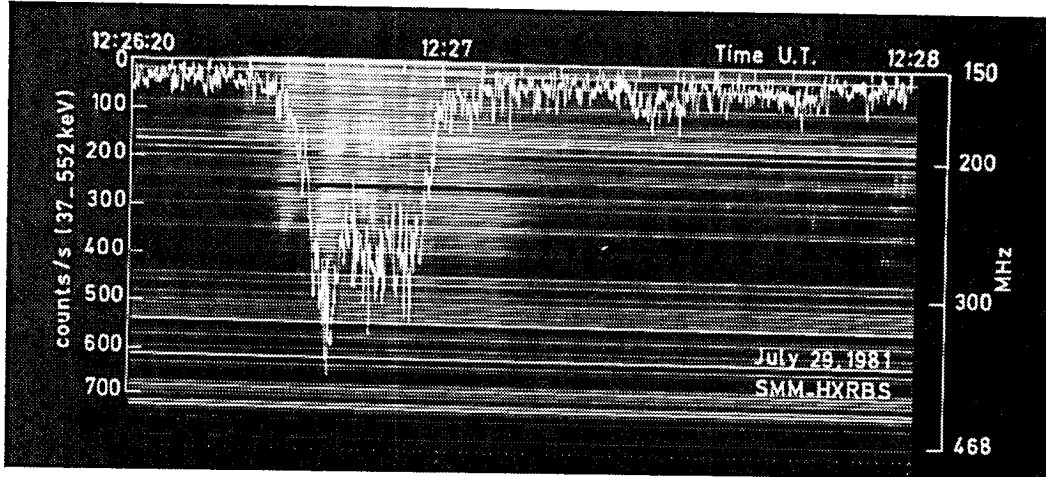


Figure 1a. Type III/V bursts on 29 July 1981 observed with the Nançay Radiospectrograph and the associated hard X-ray burst observed with HXRBS on SMM. Evolution of the X-ray emission compared to the evolution of the radio event. Note the inverted scale for the X-ray data. (From Raoult et al., 1985.)

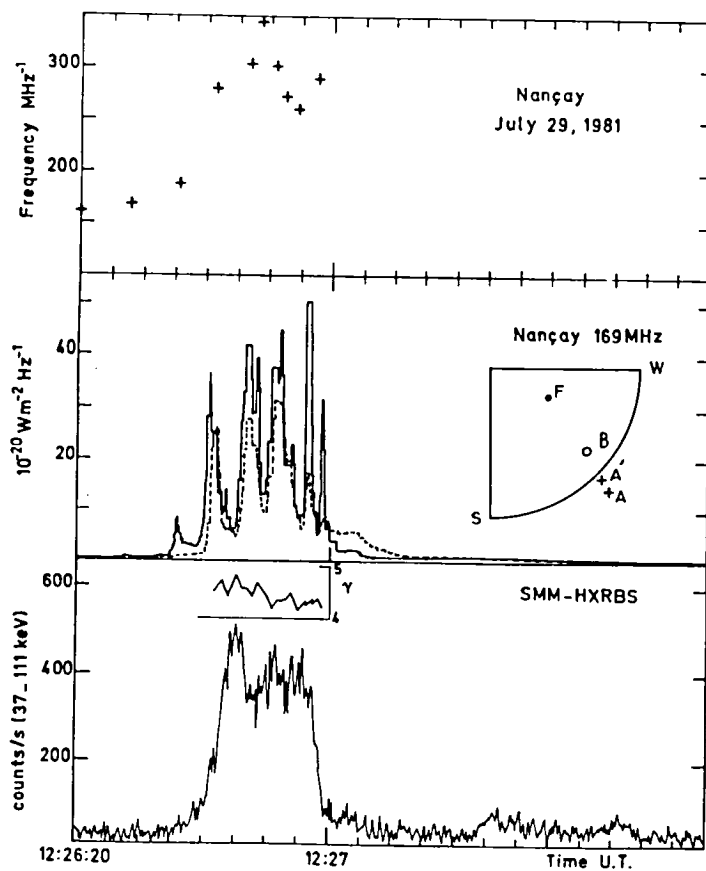


Figure 1b. 29 July 1981 event. Top: starting frequency of the radio emission measured on the Nançay digital spectrograph. Middle: evolution of the radio flux from source A' (solid line) and B (broken line) as observed by the Nançay Radioheliograph. Location of radio sources A-A' and B (see text) observed during the development of the event. Bottom: evolution of the X-ray power-law spectral index observed with the HXRBS on SMM and of the hard X-ray emission. (From Raoult et al., 1985.)

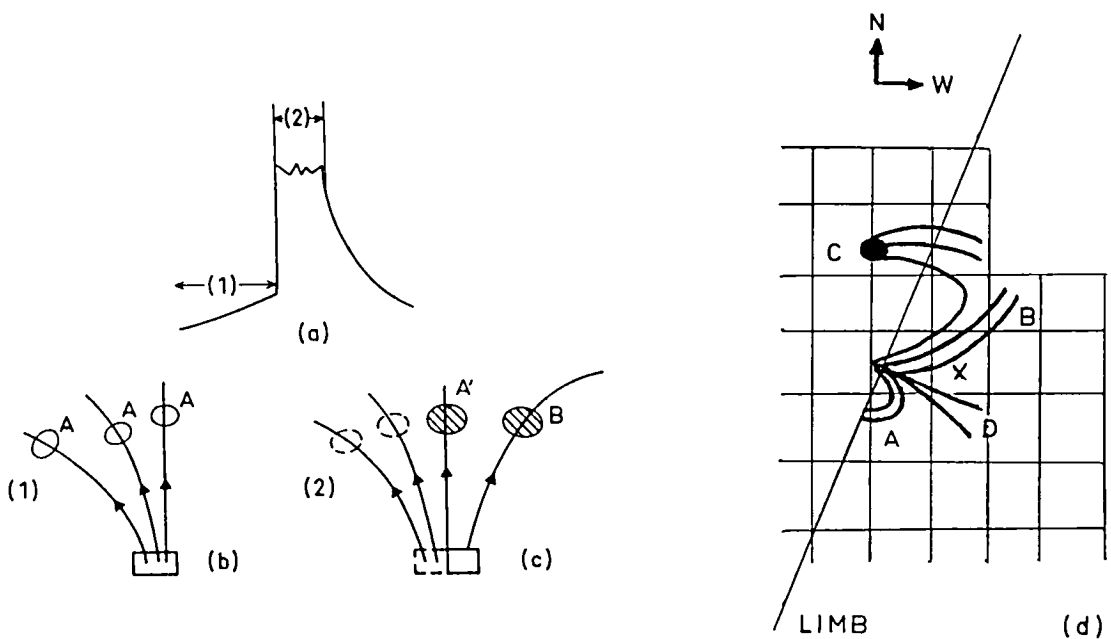


Figure 2. (a) Schematic evolution of an X-ray burst showing (1) "preflash phase," (2) impulsive phase. (b) Suggested geometry of the flare during the preflash phase showing the presumed magnetic field lines from the electron acceleration/injection site through the metric radio sources labeled A. (c) Similar geometry of the flare during the impulsive phase showing the location of the metric radio source A' and the new source B (see text). (d) 29 June event, HXIS soft X-ray data, 10.40 UT (3.5-11.5 keV). Sketch of the field geometry assumed by the authors, overlaid on a HXIS field of view display (size of individual pixels, 32 arc s). (a,b,c from Raoult et al., 1985; d from Hernandez et al., 1985) The spatial configuration suggests that the radio source B is the counterpart of the X-ray source B. (X: see caption of Figure 3).

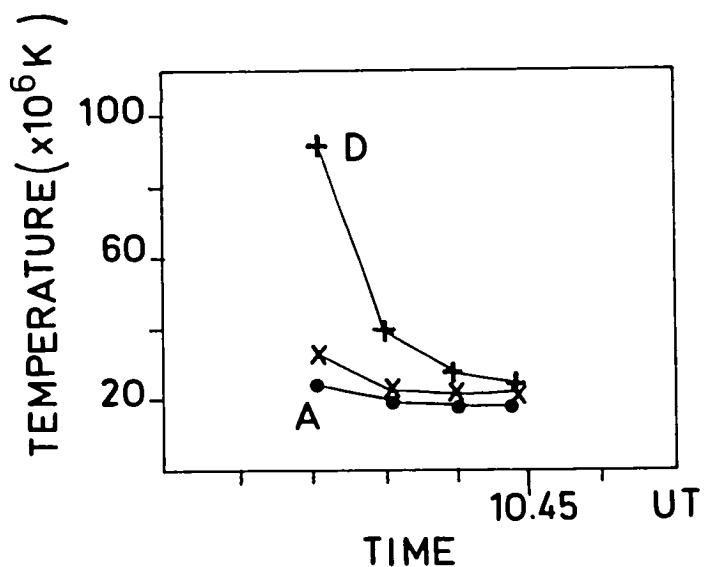


Figure 3. 29 June event 10.40 UT. Temperature versus time plots for features A, D, and its neighbor (pixel indicated by an x in Figure 2d). (From Hernandez et al., 1985.)

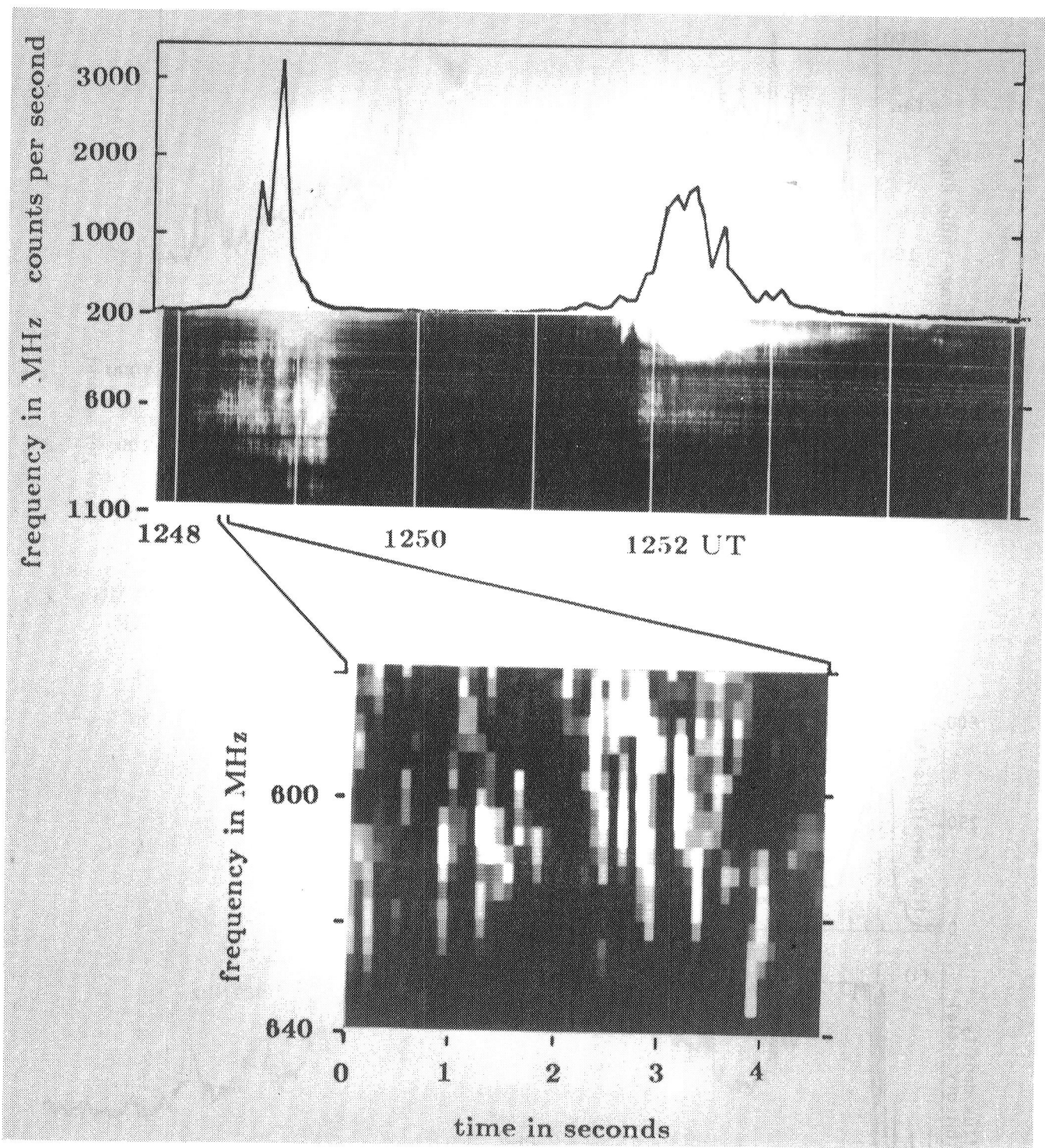


Figure 4. Decimetric spikes on 31 August 1980. Top: Composed figure showing HXR counts versus time (≥ 30 keV, observed by HXRBS onboard SMM) (courtesy B. R. Dennis) and radio spectrogram registered by the analog spectrograph (Dacedalus). The spectrogram shows type III bursts at metric wavelengths and spike activity above about 350 MHz. Bottom: Blow-up of a small fraction of the spectrogram produced from data of the digital spectrometer (Ikarus) presenting single spikes. (From Benz, 1985.)

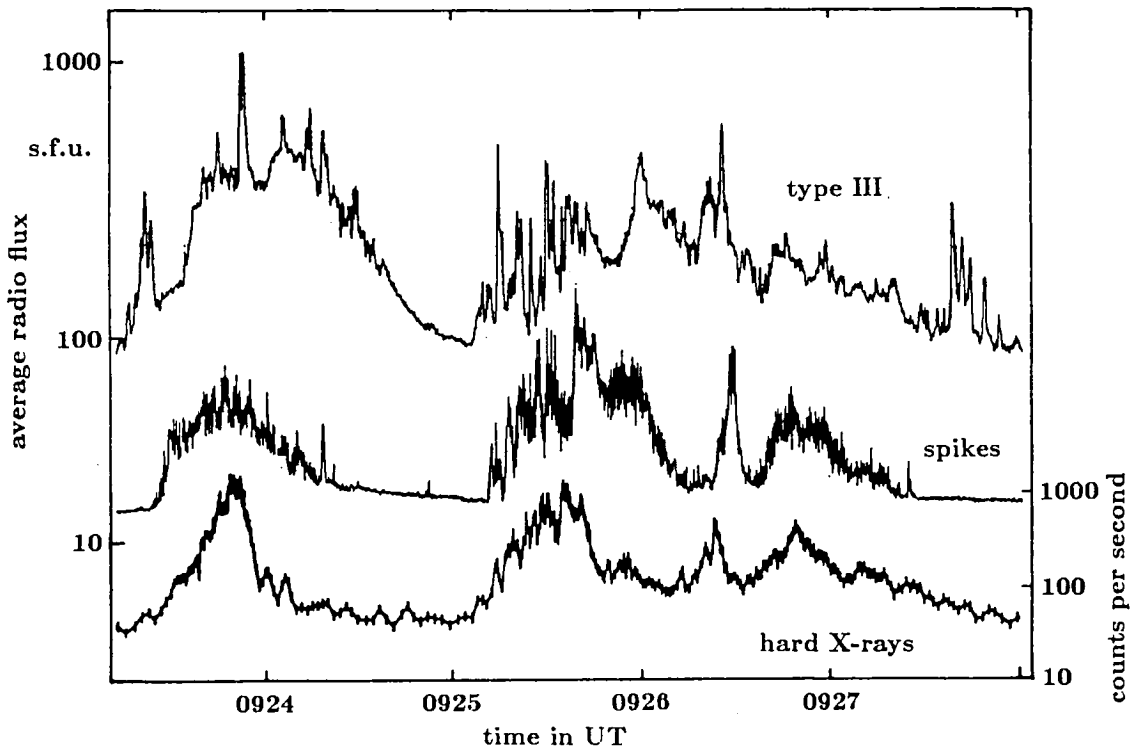


Figure 5. Correlation of average spike flux in the frequency band 580 to 640 MHz (middle) with type III emission in the 250 to 310 MHz band (top) and HXR (bottom), courtesy B. R. Dennis, HXRBS/SMM. (From Benz, 1985.)

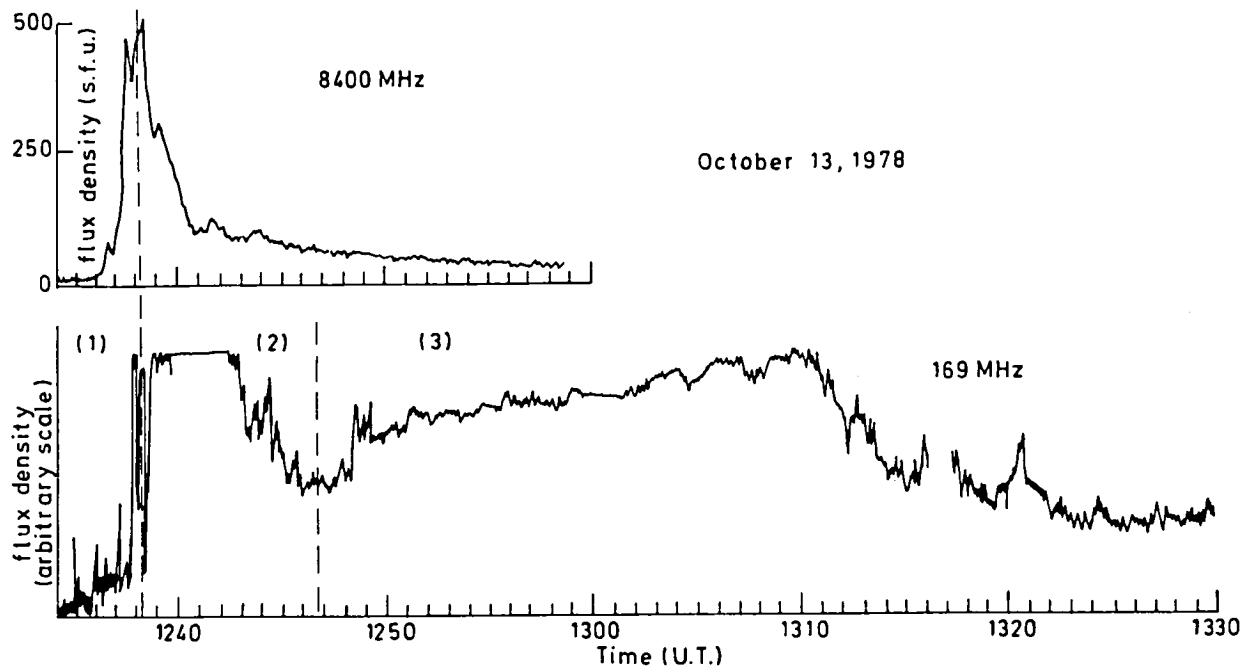


Figure 6. Time evolution of a typical event at meter wavelengths (169 MHz, Nançay) compared with the corresponding microwave event (8400 MHz, Bern). The numbers (1), (2), and (3) correspond to the impulsive phase, the flare continuum and moving type IV burst, the stationary type IV burst, respectively. (From Klein et al., 1983.)

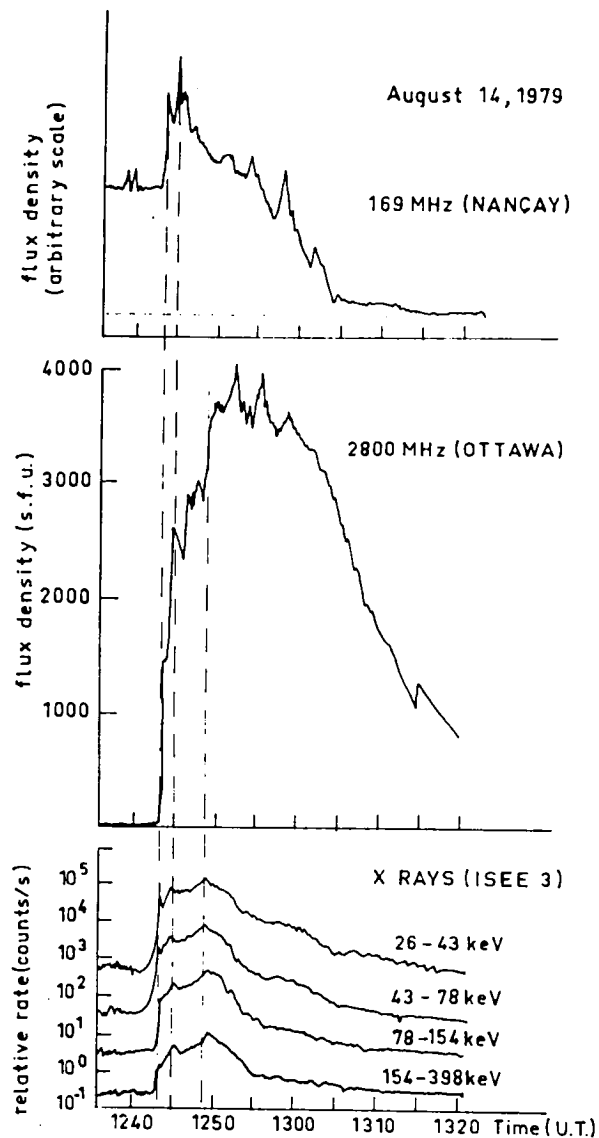


Figure 7. Time evolution of the flux densities at 169 MHz and at 2800 MHz compared with that of the hard X-ray flux (maximum fluxes: $12.0, 4.0, 2.04$ and $0.46 \text{ photons cm}^{-2} \text{ s}^{-1} \text{ keV}^{-1}$) during the 14 August event. The background level at 169 MHz is shown by the dotted line. The excess flux before the onset of the type IV burst is due to a noise storm which rose slowly from about 11:43 UT and peaked around 12:30 UT.
 (From Klein et al., 1983.)

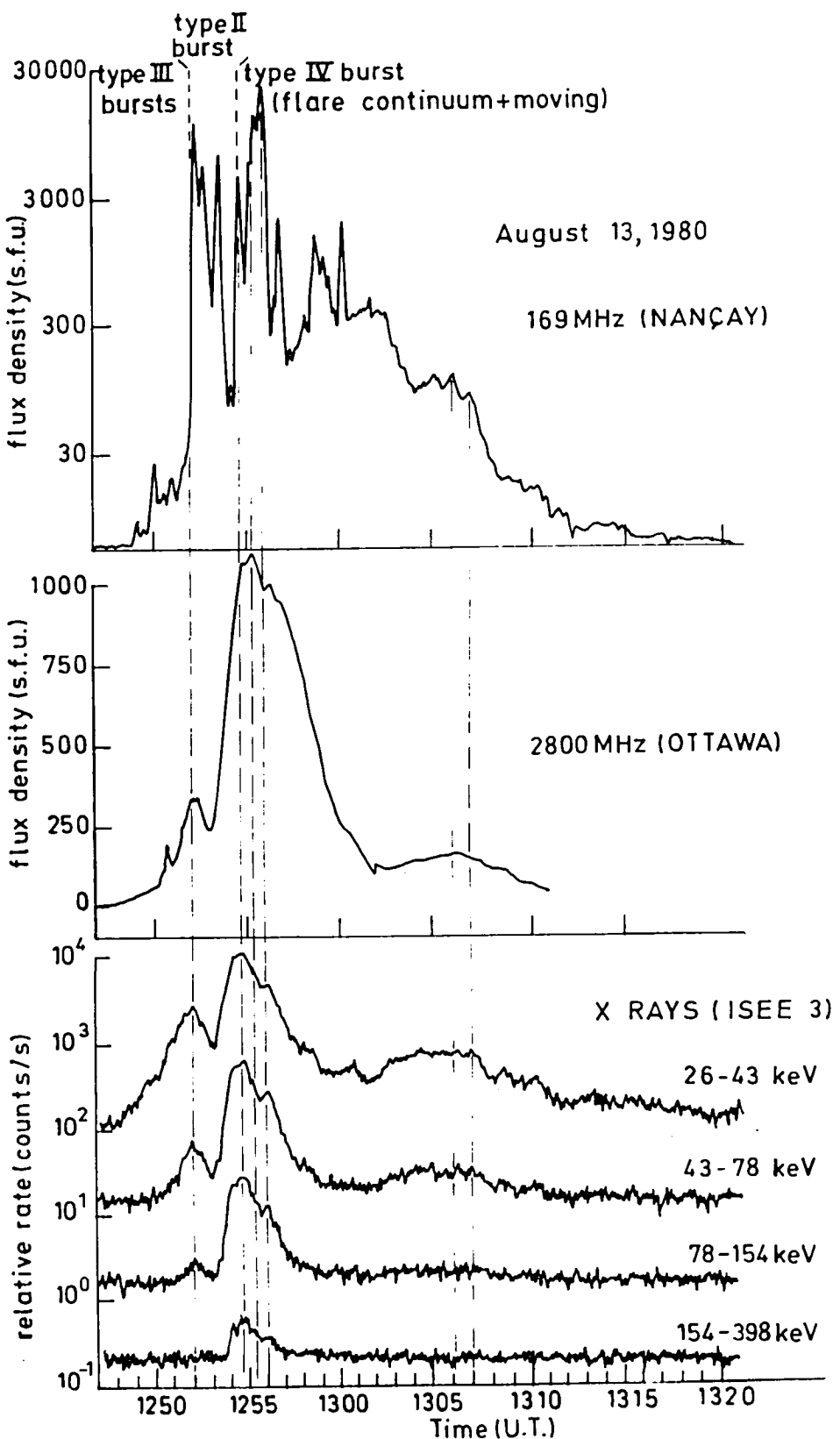


Figure 8. Same as Figure 7 for 12 August 1980 event (maximum X-ray fluxes: 6.9, 1.3, 0.33, and $0.03 \text{ ph cm}^{-2} \text{ s}^{-1} \text{ keV}^{-1}$). (From Klein et al., 1983.)

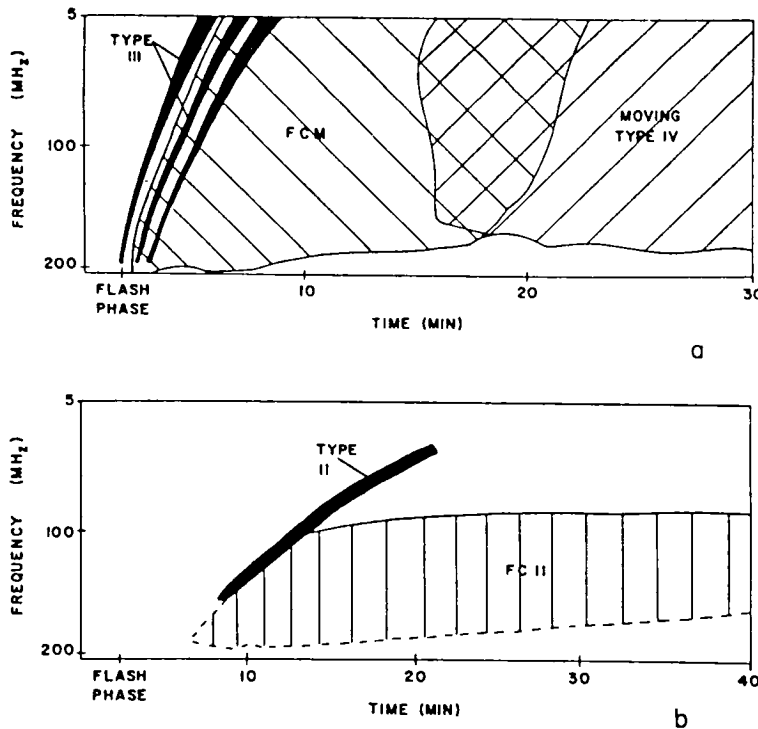


Figure 9. Schematic representation of (a) an FCM and (b) an FCII. (From Robinson, 1977.)

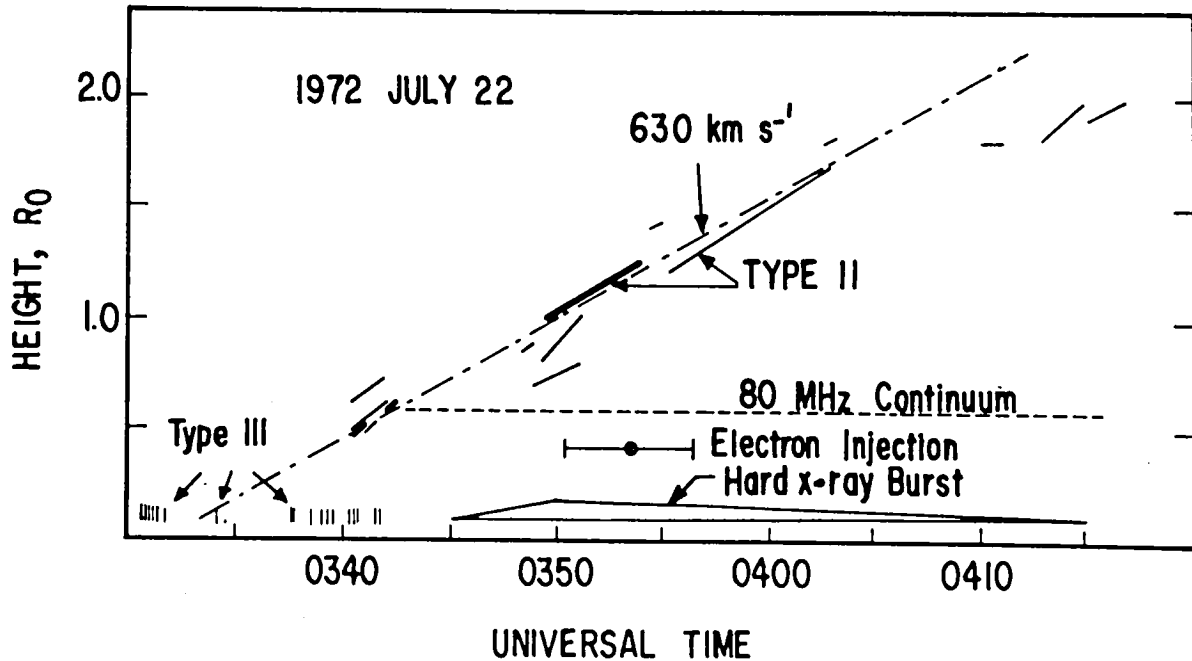


Figure 10. Height-time plot of the type II burst of 22 June 1972. Heavy sloping lines indicate (assumed fundamental) type II bands; medium sloping lines represent (assumed second harmonic) bands. The light broken line indicates a shock speed $\sim 630 \text{ km s}^{-1}$. Type II frequencies were converted to heights using the Newkirk (1961) coronal streamer density model. Also shown are the times of type III bursts (vertical bars), the flare continuum source at 80 MHz at an observed height ~ 0.6 solar radii, and the time profile of the hard X-ray burst. Error bar indicates the injection time inferred from interplanetary observations. (From Hudson et al., 1982.)

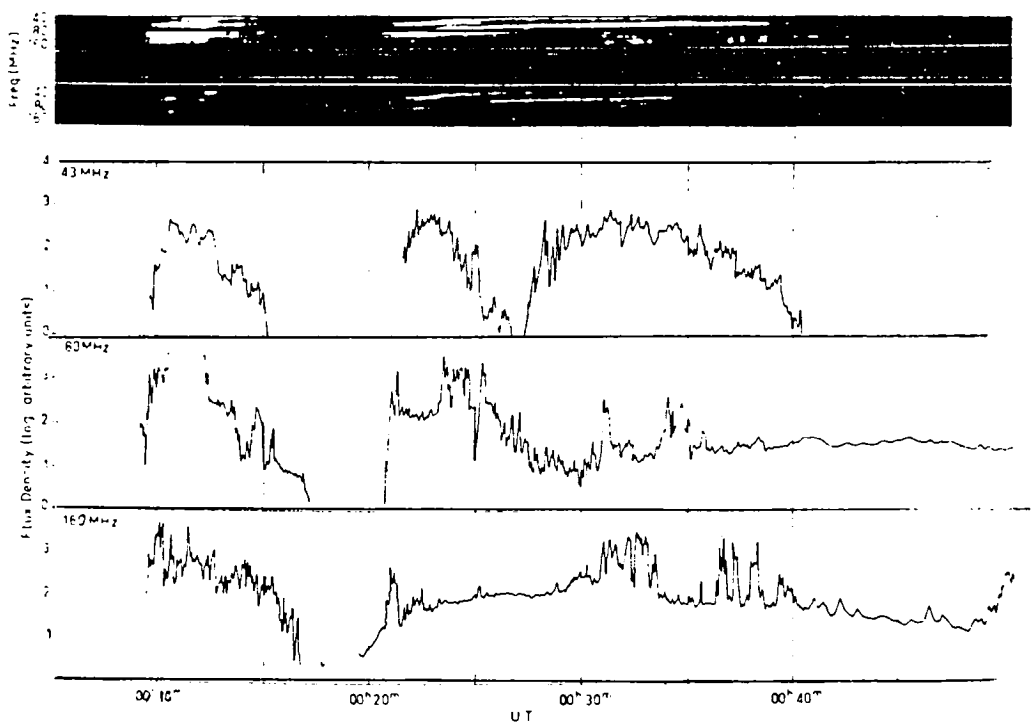


Figure 11. An FCII event which includes flash phase activity. A swept frequency spectrum and single frequency flux observations at 43, 80, and 160 MHz are given.
(From Robinson, 1977.)

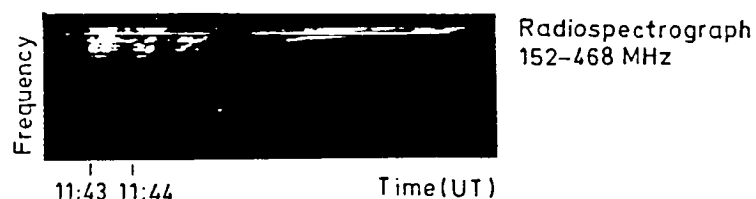
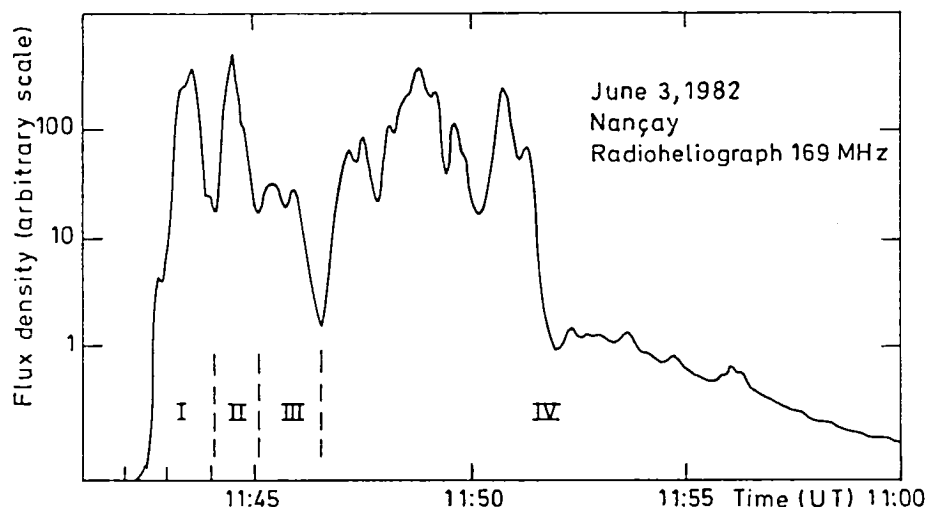


Figure 12. 3 June 1982 event. Radio observations.

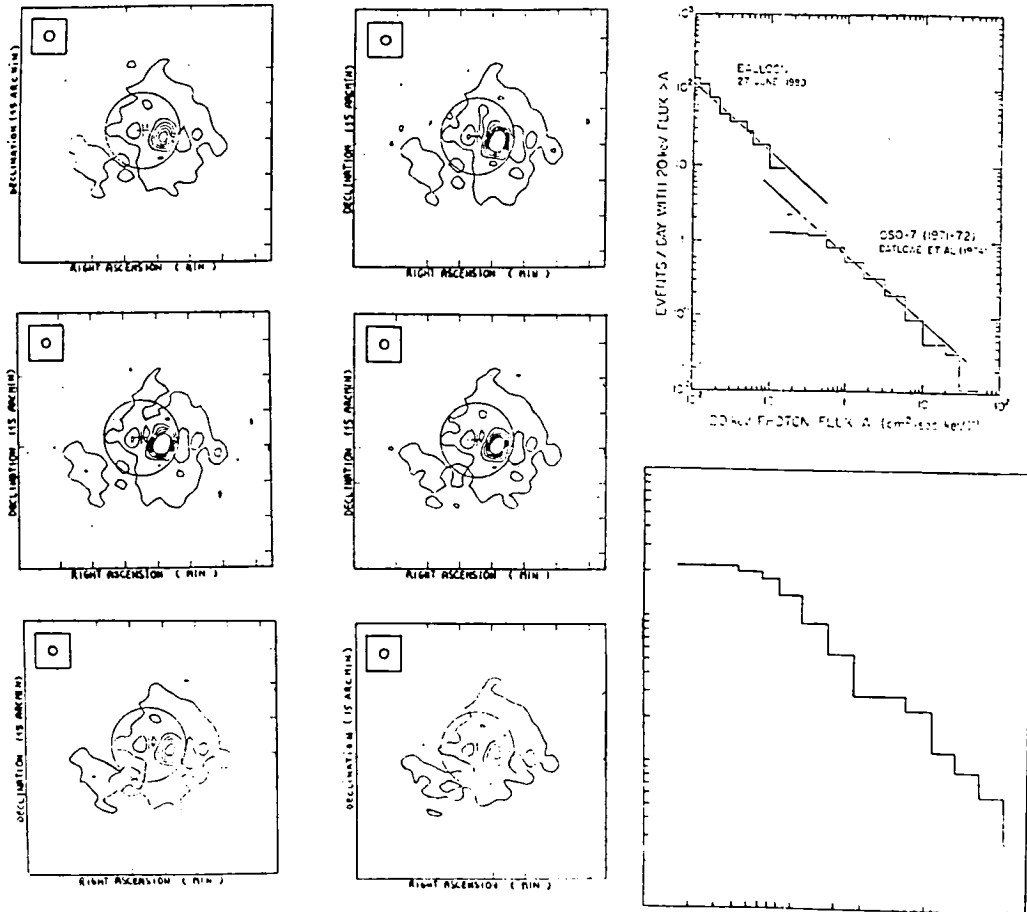


Figure 13. (left) A sequence of radioheliograms at 150 MHz showing the positions of type III-like bursts. Successive images were taken every 1 to 2 seconds. (Right top) Distribution of hard X-ray microbursts observed by Lin et al. (1984) as a function of peak keV photon flux. Also shown for comparison is the distribution of hard X-ray bursts reported by Datlowe et al. (1974). (Right bottom) Distribution of meter-decameter microbursts at 50 MHz as a function of intensity in arbitrary units. The lowest intensity is a small fraction of 1 sfu. (From Kundu and Stone, 1984.)